RESEARCH ARTICLE

WILEY

Distinguishable brain networks relate disease susceptibility to symptom expression in schizophrenia

Zhaowen Liu[1]* | Jie Zhang[2,3]* | Kai Zhang[4]* | Junying Zhang[1]* | Xiaojing Li[5,6]* | Wei Cheng[2] | Mingli Li[5,6] | Liansheng Zhao[5,6] | Wei Deng[5,6] | Wanjun Guo[5,6] | Xiaohong Ma[5,6] | Qiang Wang[5,6] | Paul M. Matthews[7] | Jianfeng Feng[2,8,9,10,11] | Tao Li[5,6]

[1]School of Computer Science and Technology, Xidian University, Xi'an, Shannxi 710071, People's Republic of China

[2]Institute of Science and Technology for Brain-Inspired Intelligence, Fudan University, Shanghai 200433, People's Republic of China

[3]Department of Medical Imaging, Jinling Hospital, Nanjing University School of Medicine, Nanjing 210002, People's Republic of China

[4]Department of Computer and Information Sciences, Temple University, 1801 North Broad Street, Philadelphia, Pennsylvania 1912

[5]Mental Health Center and Psychiatric Laboratory, The State Key Laboratory of Biotherapy, West China Hospital of Sichuan University, Chengdu, Sichuan 610041, People's Republic of China

[6]West China Brain Research Center, West China Hospital of Sichuan University, Chengdu, Sichuan 610041, People's Republic of China

[7]Division of Brain Sciences, Department of Medicine and Centre for Neurotechnology, Imperial College, London W12 0NN, United Kingdom

[8]Shanghai Center for Mathematical Sciences, Shanghai 200433, People's Republic of China

[9]Department of Computer Science, University of Warwick, Coventry, CV4 7AL, United Kingdom

[10]Collaborative Innovation Center for Brain Science, Fudan University, Shanghai 200433, People's Republic of China

[11]Zhongshan Hosipital, Fudan University, Shanghai 200433, People's Republic of China

Correspondence
Tao Li, Mental Health Center, West China Hospital, Sichuan University, Chengdu, Sichuan 610041, People's Republic of China.
Email: litaohx@scu.edu.cn and Jianfeng Feng, Institute of Science and Technology for Brain-Inspired Intelligence, Fudan University, Shanghai 200433, People's Republic of China, and Department of Computer Science, University of Warwick, Coventry CV4 7AL, United Kingdom.
Email: jianfeng64@gmail.com and Paul M. Matthews, Division of Brain Sciences, Department of Medicine and Centre for Neurotechnology, Imperial College London, United Kingdom.
Email: p.matthews@imperial.ac.uk and Jie Zhang, Institute of Science and Technology for Brain-Inspired Intelligence, Fudan University, Shanghai 200433, People's Republic of China.
Email: jzhang080@gmail.com

Abstract

Disease association studies have characterized altered resting-state functional connectivities describing schizophrenia, but failed to model symptom expression well. We developed a model that could account for symptom severity and meanwhile relate this to disease-related functional pathology. We correlated BOLD signal across brain regions and tested separately for associations with disease (disease edges) and with symptom severity (symptom edges) in a prediction-based scheme. We then integrated them in an "edge bi-color" graph, and adopted mediation analysis to test for causality between the disease and symptom networks and symptom scores. For first-episode schizophrenics (FES, 161 drug-naïve patients and 150 controls), the disease network (with inferior frontal gyrus being the hub) and the symptom-network (posterior occipital-parietal cortex being the hub) were found to overlap in the temporal lobe. For chronic schizophrenis (CS, 69

medicated patients and 62 controls), disease network was dominated by thalamocortical connectivities, and overlapped with symptom network in the middle frontal gyrus. We found that symptom network mediates the relationship between disease network and symptom scores in FEP, but was unable to define a relationship between them for the smaller CS population. Our results suggest that the disease network distinguishing core functional pathology in resting-state brain may be responsible for symptom expression in FES through a wider brain network associated with core symptoms. We hypothesize that top–down control from heteromodal prefrontal cortex to posterior transmodal cortex contributes to positive symptoms of schizophrenia. Our work also suggests differences in mechanisms of symptom expression between FES and CS, highlighting a need to distinguish between these groups.

KEYWORDS

disease association study, functional brain network, resting-state fMRI, schizophrenia, symptom association study

1 | INTRODUCTION

Resting-state fMRI is a useful tool for exploring the functional organization of the brain and has revealed differences in functional connectivity (herein called disease edges, which form the disease network) in a number of psychiatric disorders including schizophrenia (Camchong, MacDonald, Bell, Mueller, & Lim, 2011; Cheng et al., 2015a; Guo, Kendrick, Yu, Wang, & Feng, 2014; Liu et al., 2008; Zhang, Kendrick, Lu, & Feng, 2015), depression (Fitzgerald, Laird, Maller, & Daskalakis, 2008; Lui et al., 2011; Tao et al., 2013), anxiety (Cui et al., 2016; Sylvester et al., 2012; Liu, et al., 2015), autism (Cheng, Rolls, Gu, Zhang, & Feng, 2015b; Müller et al., 2011), and attention deficit hyperactivity disorder (ADHD) (Castellanos & Proal, 2012; Mazaheri et al., 2010). Among these, schizophrenia has received the greatest attention (Rosenberg et al., 2016).

However, a consensus network describing the relationships between symptom expression and brain network activity differences has been difficult to distill (Fornito, Zalesky, Pantelis, & Bullmore, 2012). We reviewed the literature again. Using "schizophrenia," "resting-state," "fMRI," and "symptom" (and their combinations) as keywords, we identified 300 articles in a search of PubMed. We found 50/300 describing correlations between altered functional connectivity (or gray matter volume) and symptom scores. Network models developed for schizophrenia most typically failed to show significant correlations with symptom scores: 13/50 found no significant correlations ($p > .05$, uncorrected), 37/50 articles reported correlations without adjusting significance threshold for multiple correlations and only 3/50 reported significant correlations with fully corrected p values ($p < .05$) (see Supporting Information, Figure S1 and Supporting Information, Table S8 for the psychopathology scales, imaging measures and corresponding p value in these papers). Several factors may have contributed to this, including the lack of simple, direct relationships between brain disease pathology, and symptom expression (e.g., because of intrinsic adaptive mechanisms; Bhandari, Voineskos, Daskalakis, Rajji, & Blumberger,

2016), heterogeneity of disease mechanisms and duration across the populations studied, the effects of treatments and small sample sizes.

For this report, we readdressed the challenge, applying a novel approach. First, rather than developing network models for a population based on *a priori* regions of interest (ROI), we have undertaken a Disease Association Study (DAS), in which edges in the network were defined based on disease associated differences in whole-brain functional connectivity (Camchong et al., 2011; Cheng et al., 2015a; Guo et al., 2014; Liu et al., 2008). Rather than using only a simple DAS, which defines pathological differences in connectivities relative to a reference (healthy) population, we extended concepts underpinning recent work of Rosenberg et al. (2016) by performing in parallel a Symptom Association Study (SAS) that searches for functional connectivities significantly correlated with the severity of symptoms of schizophrenia (symptom edges). We then integrated them to test the hypothesis that the two types of networks interact in the genesis of the expression of symptoms, i.e., that nodes in symptom network mediate relationships between disease pathology and the expression of symptoms.

We tested the hypothesis with a unique, large dataset of drug-naïve FES patients. To better understand possible sources of heterogeneity in the earlier literature, we also explored further whether these relationships change in medicated patients with chronic disease. For both datasets, we identified associated disease (by DAS) and symptom (by SAS) networks. We estimated their correlations with each other and with symptoms and created an edge-bicolor graph integrating the disease and symptom networks (in which each network is represented by a color) to define their topological coupling. We then explored relationships between disease and symptom networks and symptom expression formally with a mediation analysis.

2 | METHODS

2.1 | Subjects

The first episode schizophrenia dataset includes 358 subjects (180 controls; 178 drug-naïve patients) from Huaxi Hospital, as reported in

TABLE 1 Demographic and clinical characteristics of schizophrenia patients and matched controls in Huaxi (first episode) and Taiwan (chronic stage) datasets

	Schizophrenia patients (161)	Controls (150)	*p* value
First episode: Huaxi dataset			
Age (years)	24.03 ± 8.11	25.81 ± 8.72	.09
Education (years)	11.97 ± 3.31	13.09 ±3.26	.03
Sex (M/F)	81/79	80/70	.63
Illness duration (months) (*n* = 157)	0.99 ± 2.16	n.a.	n.a.
PANSS aggregate score (*n* = 157)	91.23 ± 16.51	n.a.	n.a.
PANSS: positive scale (*n* =157)	24.69± 5.81	n.a.	n.a.
PANSS: negative scale (*n* = 157)	19.59 ± 7.60	n.a.	n.a.
PANSS: general scale (*n* = 157)	46.97 ± 8.85	n.a.	n.a.
Chronic: Taiwan dataset			
	Schizophrenia patients (69)	Controls (62)	*p* value
Age (years)	31.6 ± 9.6	29.9 ± 8.6	.28
Education (years)	14.19 ± 2.16	15.29 ± 2.39	.06
Sex (M/F)	35/34	25/37	.24
Illness duration (years) (*n* = 69)	7.17 ± 6.61	n.a.	n.a.
PANSS aggregate score (*n* = 64)	52.81 ± 16.78	n.a.	n.a.
PANSS: positive scale (*n* =64)	11.92± 4.70	n.a.	n.a.
PANSS: negative scale (*n* = 64)	13.61 ± 6.32	n.a.	n.a.
PANSS: general scale (*n* = 64)	27.28 ± 9.63	n.a.	n.a.

previous papers (Lui, et al., 2009; Li et al., 2016). The chronic schizophrenia dataset includes 131 Taiwanese subjects (62 controls; 69 medicated patients) from National Taiwan University Hospital, also reported in a previous paper (Guo et al., 2014) (see Table 1 for detailed demographics and Supporting Information, Table S1 for drug treatments of chronic patients). All patients were identified according to DSM-IV diagnostic criteria by qualified psychiatrists, and symptom severity was assessed (Li et al., 2016) using the Positive and Negative Syndrome Scale (PANSS). Exclusion criteria included (1) presence of other DSM-IV disorders, (2) history of substance abuse, and (3) clinically significant head trauma. Using DSM-IV criteria, healthy controls were confirmed to be free of schizophrenia or other Axis 1 disorders and not to have a history of substance abuse or clinically significant head trauma. Written informed consent was obtained from all participants, and ethical guidelines were approved by the Institutional Review Boards (IRB) of the respective hospitals (mainland China and Taiwan).

2.2 | Data acquisition

For the FES dataset, functional images were collected by using a gradient-echo Echo-Planar Imaging (EPI) sequence (repetition time (TR)/echo time (TE) = 2,000/30 ms, flip angle = 90°). The slice thickness was 5 mm (no slice gap), with a matrix size of 64 × 64 and a field of view (FOV) of 240 × 240 mm^2, resulting in a voxel size of 3.75 × 3.75 × 5 mm^3. Each brain volume was comprised of 30 axial

slices, and each functional run contained 200 image volumes. During data acquisition, the subjects were instructed to keep their eyes closed but not fall asleep. In addition, high-resolution T1-weighted volumetric 3D images were obtained using a spoiled gradient recall (SPGR) sequence (TR = 8.5 ms, TE = 3.4 ms, flip angle = 12°, slice thickness = 1 mm) with an 8-channel phased-array head coil. A FOV of 240 × 240 mm^2 was used, with an acquisition matrix comprising 256 readings of 128 phase-encoding steps with 156 slices. After interpolating the T1 images in plane, the final matrix-size is 512 × 512 with an in-plane solution of 0.47 × 0.47 mm^2.

For the chronic schizophrenia dataset, all subjects underwent a structural and functional MRI scan in a single session using a 3 T MR system (TIM Trio, Siemens, Erlangen, Germany). The resting-state fMRI was performed with a gradientecho echo planar sequence. The fMRI acquisition parameters were as follows: TR =2,000 ms, TE = 24 ms, FOV = 256 × 256 mm^2, matrix 64 × 64, slice thickness 3 mm and flip angle = 90°. For each participant, 34 trans-axial slices with no gap were acquired to encompass the whole brain volume. The scan time of the resting-state fMRI was 6 min. All subjects were instructed to keep their eyes closed, but not fall asleep. In addition, a whole brain high-resolution T1-weighted MR image was acquired using a magnetization-prepared rapid gradient echo (MPRAGE) sequence (TR = 2,000 ms, TE = 2.9 ms, inversion time = 900 ms, matrix size = 192 × 256, spatial resolution = 1 × 1 mm^2, FOV = 192 × 256 mm^2, slice thickness = 1 mm without gap).

2.3 | Data preprocessing

All fMRI data were preprocessed using SPM8 (http://www.fil.ion.ucl.ac.uk/spm) and a Data Processing Assistant for Resting-State fMRI (DPARSF). The data were realigned and normalized to a standard template (Montreal Neurological Institute) and resampled to $3 \times 3 \times 3$ mm^3. All fMRI time-series underwent band-pass temporal filtering (0.01–0.08 Hz), nuisance signal removal from ventricles, deep white matter, 6 rigid-body motion correction parameters. Global signal regression, which regressed out the averaged time series over all voxels in the brain from the fMRI time-series, is still a long-lasting controversial procedure in the preprocessing of fMRI data. Different confused and contradictory guidelines are provided in the literatures (Fox, Zhang, Snyder, & Raichle, 2009; Murphy, Birn, Handwerker, Jones, & Bandettini, 2009; Murphy & Fox, 2017). Although GSR may lead to downward shift of the distribution of correlations to a mean correlation of zero (which also found in our two datasets and shown in the Supporting Information, Figure S2), it can help remove non-neuronal sources of global variance and help improve the consistency of functional connectivities within-subject across scans (Song et al., 2012). In our study, the GSR was adopted, as the raw data processed with GSR has better generalization performance using our model (the results without GSR were given in the Supporting Information for comparison). Finally, we implemented additional careful volume censoring (scrubbing) movement correction as reported by Power et al. (2014) to ensure that head motion artifacts are not driving observed effects. The mean framewise displacement was computed with framewise displacement threshold for displacement being 0.5 mm. In addition to the frame corresponding to the displaced time point, one preceding and two succeeding time points were also deleted to reduce the "spill-over" effect of head movements. Subjects with more than 10% displaced frames flagged were completely excluded from the analysis as it is likely that such high-level of movement would have had an influence on several volumes. After quality control (excluding subjects with poor imaging quality by manually checking and that with large head motion), first-episode dataset has 150 controls and 161 patients left and the chronic dataset has 62 controls and 69 medicated patients left. A detailed discussion of global signal removal and data scrubbing are also provided in the Supporting Information, Methods. 90 regional time series then were extracted by averaging voxel time series within each anatomically defined region (using the Automated-Anatomical-Labeling template (Tzourio-Mazoyer et al., 2002), and the names of the ROIs and their corresponding abbreviations are listed in Supporting Information, Table S2). From these, a whole-brain functional network (90×90) was constructed for each subject which included 4005 functional connectivities based on Pearson correlations between regional BOLD signals in the individual ROIs used as a basis for describing nodes in the brain network. All the 4005 FCs (both positive and negative) were used in following analysis.

## 2.4 | Bicolor graph construction: Disease and symptom networks

An *edge-bicolor* graph is constructed from separately generated disease and symptom network graphs. A disease network is defined through a Disease Association Study (DAS). It represents connectivities differentially expressed in people with the disease of interest relative to people who are healthy. A symptom network is defined through a Symptom Association Study (SAS), which defines correlations between brain connectivities and symptoms amongst patients with the disease of interest. For constructing the both DAS and SAS, we used "leave-one-out" cross-validation (i.e., single subjects were selected iteratively to test the performance of a model trained with data from the remaining subjects in each leave-one-out trial within a set, the size of which was identical to that of the total population available) to maximize the stability of their edges (Rosenberg et al., 2016) and to avoid the "double dipping" problem (Dubois & Adolphs, 2016). Finally, the edge-bicolor graph was built as the overlap of edges defined in the two different kinds of networks.

In this instance, to construct a DAS, whole brain connectivity data from the schizophrenia patients and from matched healthy controls were used to build classifiers distinguishing the two groups. First, the area under the receiver operating characteristic (ROC) curve (AUC) was employed to represent predictive power for each of the 4005 edges (by using the MATLAB function "rankfeatures" with age, sex, root-mean-square displacements of head movement and education years as covariates). Further, to build the optimal classifier, we changed the AUC threshold ($AUC_{threshold}$), which was used to select disease-related edges, from 0.6 to 0.8 in steps of 0.05. Under each $AUC_{threshold}$, suprathreshold edges were identified and separated into two groups: edges characterizing stronger functional connectivities in patients than in controls (increase edges) and the reverse (decrease edges). The sum of these edges for each group was expressed as the classification "strength" for that subject. The strengths of the two groups were fed into a logistic linear regression model with age, sex, root-mean-square displacements of head movement and education years as covariates to test the potential for prediction of disease state for each $AUC_{threshold}$ using the "leave-one-out" method. Performance was assessed serially across each threshold step as the area under the curve (AUC) of the receiver operating characteristic (ROC) curve; the optimal $AUC_{threshold}$ was determined by selecting the threshold that produced the highest AUC across all such "leave-one-out" trial sets (Figure 1; i.e., highest classification accuracy in all "leave-one-out" trials). We selected those edges (increased or decreased edges) appeared in each leave-one-out trail under the optimal $AUC_{threshold}$ to form the disease network.

We adopted a similar "leave-one-out" procedure to define optimal symptom edges (SAS) using the whole brain functional connectivities and the corresponding global symptom scores from each of the schizophrenia patients. We calculated the partial correlation coefficient between each functional connectivity and associated patient symptom score across patients with age, sex, root-mean-square displacements of head movement, and education years as covariates and obtained the corresponding p value. We iterated p value thresholds ($p_{threshold}$) from 0.0005 to 0.01 in steps of 0.0005. Edges with p values smaller than the $p_{threshold}$ were identified and divided into two groups that were either positively or negatively
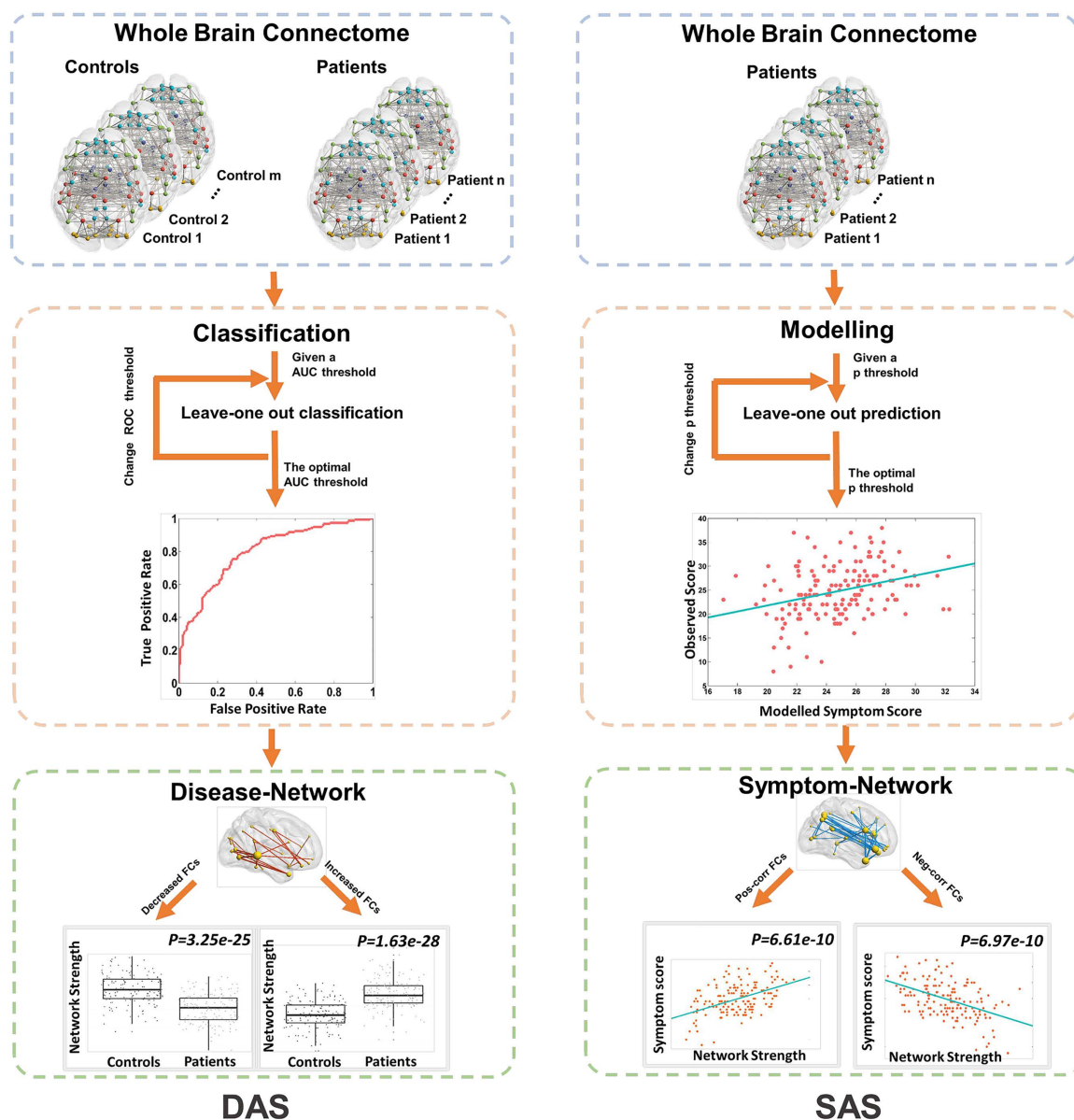
FIGURE 1 Flow chart of DAS (left) and SAS (right) approach in identifying disease edges and symptom edges in schizophrenia patients [Color figure can be viewed at wileyonlinelibrary.com]

correlated to the symptom scores. The sum of edges for each group then was used as the independent variable to fit a linear regression model with the symptom score as the dependent variable, and age, sex, root-mean-square displacements of head movement, and education years as nuisance covariates. We iteratively ran "leave-one-out" trials m times (m is the number of patients) for each $p_{threshold}$, to derive a patient-specific prediction score. The optimal $p_{threshold}$ was selected as that producing the highest correlation between real and predicted symptom scores (Figure 1). We selected those edges appeared in each leave-one-out trail under the optimal $p_{threshold}$ to form the symptom network.

After identifying the disease network and symptom networks, we then constructed an edge-bicolor graph G that included both networks. The edges of the bicolor graph consisted of two parts: $L = \{L_{disease}, L_{symptom}\}$, where $L_{disease}$ and $L_{symptom}$ refer to the disease and symptom

edges, respectively. The vertices of the bicolor graph therefore also consisted of two parts: $V = \{V_{disease}, V_{symptom}\}$, where V_{diff} denotes the vertices associated with the disease network, and $V_{symptom}$ represents the vertices of the symptom network.

To show qualitatively the difference of the correlations between the disease network and the symptom network with the symptom score, we explored the variance in symptoms that is explained by disease network and symptom network in two separate regression models. With the symptom score being the dependent variable, the sum of the increased/decreased edges in disease network, and the sum of the positively/negatively related edges in symptom network were used as the independent variables in the respective regression model. An adjusted R^2 (coefficient of determination) was used to express the proportion of the symptom score that could be explained by the model.

——————————————

2.5 | Significance of the prediction results: Permutation analysis

To determine whether the classification accuracy and predicted scores, we obtained from our DAS and SAS are significantly better than random, the nonparametric permutation procedure was adopted. For the DAS analysis, in each permutation, we randomly shifted the labels (patient or control) of participants and ran the DAS analysis to obtain the highest AUC. The null distribution for the highest AUC is formed by running the permutation procedure 1000 times. Based on the null distribution, the p value was obtained. For the SAS analysis, in each permutation run, we randomly shifted the scores across the patients and ran the SAS analysis to obtain the highest correlation between the real scores and predicted scores. We also ran the permutation procedure 1000 times to obtain the null distribution for the highest correlation between the predicted scores and the real scores. The p value of our prediction results was then obtained base on the null distribution.

2.6 | Overlap between nodes in disease and symptom networks: Permutation analysis

Finally, an additional permutation analysis was adopted to show that the overlap of nodes between disease and the symptom networks were significantly larger than the random case. In each permutation run, we randomly selected the same number of edges as the disease and symptom networks form the whole network and calculated the number of the associated nodes common to the randomly selected disease and symptom network. We ran the permutation 10,000 times to form the null distribution of the number of the overlapped nodes between the two networks. The p value was then obtained based on the null distribution.

2.7 | Mediation analysis between the disease and symptom networks and symptom expression

To further explore the mechanism that underlies the correlation between the disease network, symptom network and the symptom scores, mediation analysis, which tests whether a covariance between two variables (X and Y) can be explained by a third variable (M) was used. Here, the standard 3-variable path model (Baron & Kenny, 1986) was employed. We showed our model in Figure 4a. Our hypothesis is that the symptom networks may mediate the relationship between the disease networks and the symptom score. In the model, we used the sum of disease edges in the disease networks as the variable X, the symptom scores as Y and the sum of edges in the symptom networks as M. Path a is the estimated linear relationship between X and M. Path b is the linear M–Y relationship controlling for x. Path c represents the overall X–Y relationship and the c' path is the direct X–Y effect controlling for the M. The significance of the difference (c–c'), which can be regard as the mediation effect, can be tested by assessing the significance of the product of the path coefficients a×b (Wager, Davidson, Hughes, Lindquist, & Ochsner, 2008). Age, sex, root-mean-square displacements of head movement, and education years were served as the covariates in all of our mediation analysis.

For the FES patients, as positive symptom score was used to obtain the symptom networks, we used the positive symptom score as variable Y in the model. As for the chronic patients, the symptom network is for the negative symptom score, so we used the negative score as Y. For each of the dataset, as two disease networks (increased/decreased disease network) and two symptom networks (positively related/negatively related disease network) were obtained from our DAS and SAS analysis. We used one of the two disease networks as X and one of the two symptom networks as M, which resulted in 4 possible combinations (2 × 2). Thus, there are four different models for each dataset (see Figure 4b,c for details). Then, the accelerated, bias-corrected bootstrap test (Efron & Tibshirani, 1993) with 10,000 bootstrap samples was used to test the significance of a, b, and a×b path coefficients, respectively. If all of the paths, that is, a, b, and a×b path are significant, we can confirm our hypothesis that the relationship between the disease network and the symptom are mediated by the symptom network. All the mediation analyses were performed using the MATLAB Multilevel Mediation and Moderation (M3) Toolbox (https://github.com/canlab/MediationToolbox).

3 | RESULTS

We studied two large cohorts of schizophrenia patients and age- and sex-matched controls (Table 1). FES (mean, 24 years old) had an illness duration of less than a month and were drug-naive, while CS patients (mean, 31 years old) had a mean duration of illness in excess of 7 years (mean, 7.2 years).

3.1 | The disease network and the symptom network

For the FES dataset, the optimal $AUC_{threshold}$ in DAS analysis was found to be 0.63, which led to an AUC of 0.81 for the test set; 75.47% of patients and 71.81% of health controls were correctly classified. The nonparametric permutation analysis was used to test the significance of the AUC we obtained. One thousand times of random permutation were performed and resulted in significance at $p < .001$ (see Supporting Information, Figure S3a for more details). The disease network identified under the optimal $AUC_{threshold}$ included 57 edges (19 from relative increases and 38 from decreases). The optimal SAS analysis $p_{threshold}$ was .02, which achieved a correlation of $r = .30$ between predicted and real symptom scores ($p = 1.36 \times 10^{-4}$). The nonparametric permutation analysis was used to test the significance of the correlation between our predicted symptom scores and real scores. One thousand times of random permutation were performed and resulted in significance at $p = .003$ (see Supporting Information, Figure S3a for more details). The associated symptom network included 28 edges (11 correlated positively and 17 correlated negatively with the positive symptom scale). Note that our classification accuracy is not the highest amongst literatures, as the goal here is to determine the optimal $AUC_{threshold}$ so that the disease network can be properly identified, rather than to obtain the highest classification accuracy. A higher accuracy could be obtained by using multiple imaging modalities and optimizing feature-selection strategies and classification schemes.

For the CS dataset, the optimal $AUC_{threshold}$ in the DAS analysis was 0.75. The resulting AUC is 0.85 in the test dataset allowed 78.26% of patients and 80.65% of health controls were classified correctly. One thousand times of nonparametric permutation were performed to test the significance of our AUC, resulting in a p value $< .001$ (see Supporting Information, Figure S3b for more details). The disease network identified under the optimal $AUC_{threshold}$ included 19 edges (11 increase and 8 decrease edges). The optimal $p_{threshold}$ was 0.03 for the SAS analysis, under which the correlation between the predicted and the real symptom score is $r = .64$ ($p = 2.03 \times 10^{-8}$). One thousand times nonparametric permutation was performed to test the significance of the correlation, resulting in a p value $< .001$ (see Supporting Information, Figure S3b for more details). The symptom network obtained consisted of 68 edges (17 positively and 51 negatively correlate with the schizophrenia score).

3.2 | Characterizing schizophrenia patients with a disease network

The disease network for FES patients identified a wide range of differences in strengths of edges defined by functional connectivities relative to the matched healthy volunteers. Major differences were found for connectivities between the prefrontal (orbitofrontal and inferior frontal cortex, and the medially adjacent rectus gyrus) and the parietal (precuneus and angular gyrus) and temporal (temporal pole) cortices and the thalamus (Figure 2a and Supporting Information, Table S3). By contrast, the disease network for the CS cohort identified major differences in functional connectivities between the thalamus and middle and superior prefrontal cortices and the postcentral gyrus (Figure 3a and Supporting Information, Table S5).

3.3 | Symptom networks highlight functional connectivities distinct from those in the disease networks

For FES, the symptom network was defined by associations with positive symptoms. These defined edges between the middle temporal gyrus or temporal pole and both the occipital lobe (lingual, calcarine, and fusiform gyri) and midline cingulate cortex (middle cingulate gyrus) (Figure 2b and Supporting Information, Table S4). By contrast, for the CS patients, the symptom network was related to negative symptoms and prominently involved functional connectivities between the occipital (calcarine, lingual, and fusiform gyri) and the parietal (posterior cingulate gyrus, pre/postcentral gyrus) and temporal (Heschel's, middle, and temporal gyri) cortices (Figure 3b and Supporting Information, Table S6).

3.4 | Common nodes relate disease and symptom networks

The bicolor graph representation facilitates description of common nodes (topological coupling) relating the disease and symptom networks (Figures 2 and 3). For the FES patients, this highlighted common nodes in the temporal (temporal pole, middle temporal gyrus) and calcarine cortex. As seen in Figure 2c, these regions are hubs in both networks (nodes with large number of both disease and symptom edges). A different set of functional connectivities better described the overlap between disease and symptom networks for CS patients (Figure 3c). This highlighted the thalamus and postcentral gyrus as common hubs. The permutation analysis showed that the number of overlapping nodes between the disease and symptom networks were significantly higher than chance ($p = .0002$ and $.0001$ for FES and CS, respectively).

3.5 | Symptom networks better explain schizophrenic symptoms than do disease networks

As expected, symptom edges showed stronger correlations with symptom scores than did disease edges (Supporting Information, Figure S4a), although they did not distinguish patients from controls well (Supporting Information, Tables S4 and S6). For FES patients, the positive symptom score was significantly higher than the negative score ($p = 2.12 \times 10^{-37}$) and the prediction accuracy for the positive score is significantly better than that of the negative score $p = 2.43 \times 10^{-4}$, see Supporting Information, Figure S5a for details. The symptom network explained over 2.5-fold more variance in symptoms across the cohort (29%) than did the disease network (12%). For the patients with chronic schizophrenia, the negative symptom score was higher than the positive symptom score ($p = 7.88 \times 10^{-8}$) and the prediction accuracy for the negative score is significantly better than that of the positive score ($p = .0418$, see Supporting Information, Figure S5b for details). Again, the symptom network could explain greater than 2.5-fold more of the variance in symptoms (50%) than the disease network (19%) (Supporting Information, Figure S4b).

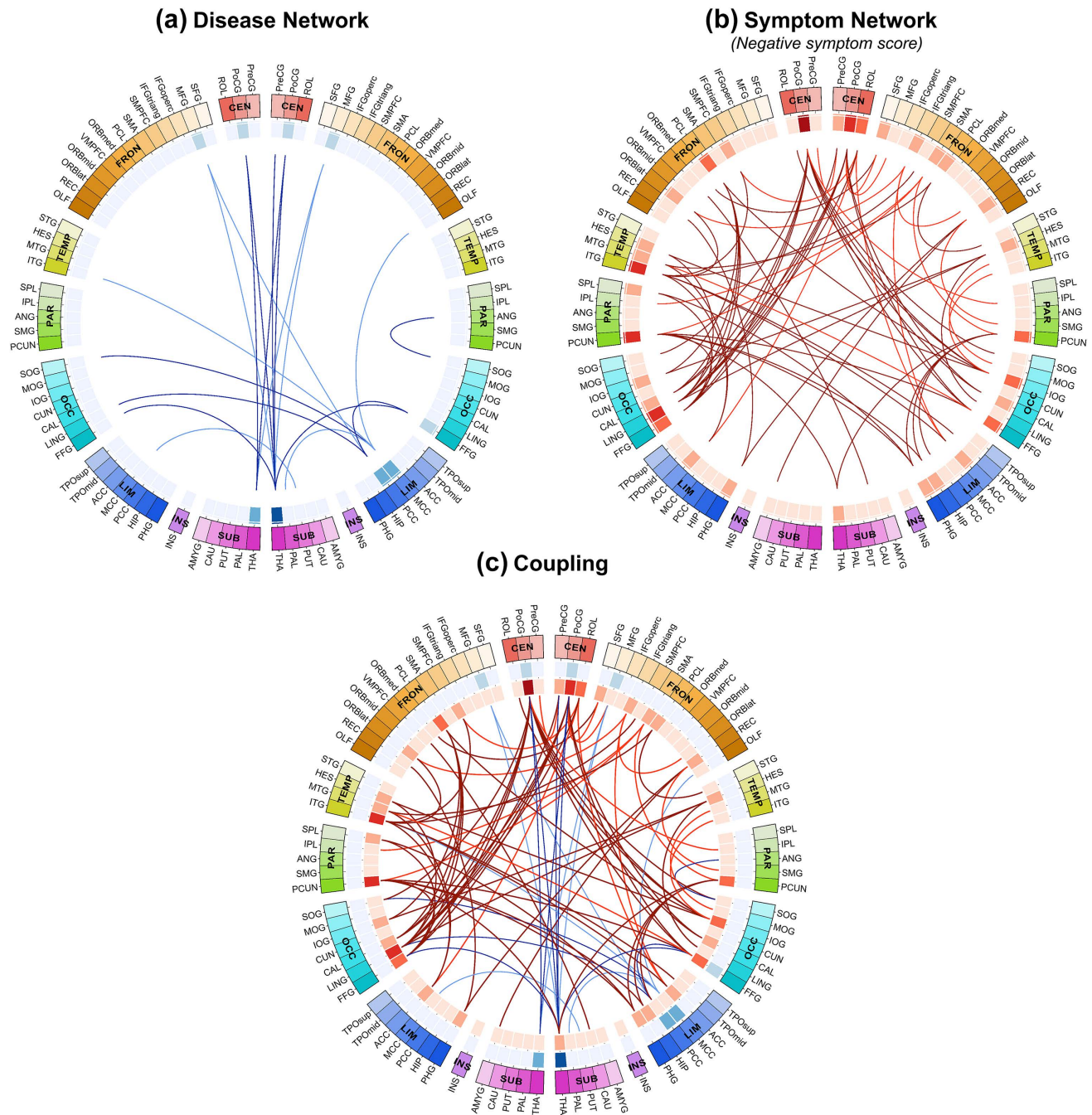## 3.6 | Symptom networks mediate relationships between disease networks and symptoms

Disease and the symptom network edges showed strong correlations in the FES patients (Supporting Information, Table S7a). We tested for relationships with symptom expression formally using mediation analysis. For the FES patients, we found evidence supporting a model in which the symptom network mediates relationships between functional connectivity differences associated with disease and symptom expression. We tested all four possible combinations involving the sum of increased/decreased disease edges, the sum of positively related/negatively related symptom edges, and positive symptom score and found significant mediation effect of the symptom network on the relationships between disease network and the expression of positive symptoms of schizophrenia with path a, b, and a×b are significant for all four models (Table 2). However, we were unable to demonstrate a similar relationship for the chronic state patients with negative symptoms (Table 3). For this cohort, the correlation between the disease and symptom networks is lower (Supporting Information, Table S7b) and a significant relationship between the disease and symptom networks and symptom scores was not found (Figure 4b). In addition, we also tested the significance of another possible mediation model (the

First-episode Schizophrenia

FIGURE 2 Disease network and symptom network identified in FES patients, which were shown in an edge-bicolor graph, with disease edges represented by blue and symptom edges by red. The disease network consists of functional connectivities significantly changed in FES patients compared to matched controls (including all increased and decreased disease edges identified in DAS) (a, see Supporting Information, Table S3) and the symptom network consists of functional connectivities significantly correlated with positive PNASS scores of FES patients (including positively-related and negatively-related symptom edges identified in SAS) (b, Supporting Information, Table S4. The topological coupling between the disease network and symptom network are shown in c, which is the integration of a and b. The color of the outside circle denotes the 90 different automatic anatomical labelling (AAL) regions. The color of the inside circle denotes the number of edges of the corresponding node (deep color means a hub node). In a, deep and light blue indicates increased and decreased disease edges in patients compared to controls. In b, deep and light red indicates negatively and positively related symptom edges (with positive symptom scores) in patients. [Color figure can be viewed at wileyonlinelibrary.com]

symptom mediates the relationship between the disease network and symptom network) in the FES dataset and did not found significant mediation effect, details in Supporting Information, Figure S7 and Table S9.

4 | DISCUSSION

Here we have characterized disease network and symptom network for populations of patients with schizophrenia of two different stages.

FIGURE 3 Disease network (including all increased and decreased disease edges identified in DAS) and symptom network (including positively related and negatively related symptom edges identified in SAS) identified in chronic schizophrenia patients, which were shown in an edge-bicolor graph, with disease edges represented by blue and symptom edges by red. The disease network and the symptom network (consisting of functional connectivities that are correlated with negative symptom score) are detailed in Supporting Information, Tables S5 and S6, respectively [Color figure can be viewed at wileyonlinelibrary.com]

We discovered distinct networks for distinguishing the patients with medication naïve, first episode schizophrenia, and those patients with chronic disease on treatment. These differences suggest disease stage or medication as important sources of variance in developing these models. However, even with control for this heterogeneity, disease networks did not explain much of the variance in symptom expression amongst patients in either group. Symptom networks described this better for both the FES and CS patients. Bicolor graphs relating disease and symptom networks identified common hubs for each population. A formal mediation analysis suggested that the symptom network mediated relationships between the disease network and symptom expression for the first episode schizophrenics, who displayed predominantly

TABLE 2 Mediation analysis results for the hypothesis that symptom networks mediate the relationship between the disease network and the positive symptom in first-episode dataset

X	M	Y	a path		b path		ab path	
			Z	p	Z	p	Z	p
Increased disease network	Positively related symptom network	Positive score	−3.89	<.0001	3.95	<.0001	3.95	.0002
Increased disease network	Negatively related symptom network	Positive score	2.77	.0057	−3.66	.0003	−2.70	.0068
Decreased disease network	Positively related symptom network	Positive score	3.46	.0005	4.08	<.0001	3.79	.0002
Decreased disease network	Negatively related symptom network	Positive score	−3.82	<.0001	−3.58	.0003	3.94	<.0001

positive symptoms of the disease, although this could not be shown for the predominantly negative symptoms of the chronic-stage patients.

Our work highlights differences in the functional connectivity models between those that best classify resting state BOLD signals in patients relative from a healthy population and those needed to explain the variance in symptoms in the patient population. For both FES and CS patients, differences in functional activity in prefrontal cortices contributed prominently descriptions the disease networks. This is consistent with considerable literature suggesting dysfunctional striatal-prefrontal interactions as core aspects of the functional pathology of the disease (Howes & Kapur, 2009; Simpson, Kellendonk, & Kandel, 2010). However, a network involving heteromodal temporal cortex and parietal-occipital regions best explained positive symptom expression in the first episode cohort.

Relationships between these alternate representations of functional pathology associated with schizophrenia were highlighted in the bicolor graphs. For FES patients, the two networks intersected most prominently in middle temporal pole and middle temporal gyrus (Figure 2c). The left temporal pole previously was proposed as an important heteromodal hub for recognition and naming (Tranel, 2009) and is the locus of convergence of language streams (Spitsyna, Warren, Scott, Turkheimer, & Wise, 2006), while the activation in left middle temporal gyrus is associated with hallucinations (Lennox, Bert, Park, Jones, & Morris, 1999; Onitsuka et al., 2004). These functionally connected regions also are anatomically connected; the arcuate fasciculus provides a putative structural basis for disease edges (between interior frontal gyrus and middle temporal gyrus/temporal pole). Reduced integrity of the arcuate fasciculus is associated with auditory and verbal hallucinations (McCarthy-Jones, Oestreich, Whitford, & Bank, 2015). Arguing analogously, the inferior longitudinal fasciculus provides a possible structural basis for the symptom edges

between middle temporal gyrus/temporal pole and lingual/calcarine gyrus.

The correlations between disease and symptom networks that we have found are consistent with the hypotheses that the variation in functional differences between patients and healthy volunteers are associated for the range of symptom expression in the patient population. For FES patients, the disease edges connecting interior frontal gyrus and middle temporal gyrus/temporal pole correlate negatively with symptom edges that connect middle temporal gyrus/temporal pole and lingual/calcarine gyrus (Figure 2c) and these symptom edges, in turn, correlate negatively with positive symptoms, mainly delusion and hallucination (Supporting Information, Figure S6). From these relationships defined between disease edges and positive symptom via symptom edges (Figure 4a), we predict that increases in specific disease edge (frontal–temporal connectivities) strengths will lead to more severe positive symptom. However, further work will be needed to test the generalizability and predictive utility of these models.

The associations between disease edges associated with inferior frontal gyrus, symptom edges associated with posterior sensory processing areas in the occipital and parietal cortex, and positive symptoms like delusion and hallucination illustrate how these models can suggest hypotheses regarding causal mechanisms. For example, the anterior–posterior interactions suggests that prefrontal executive dysfunction may contribute "top down" to the pathological sensory processing responsible for positive symptoms in FES (Allen, Laroi, McGuire, & Aleman, 2008; Biederman, Glass, & Stacy, 1973). Such a model emphasizes a central importance for pathological functions of the prefrontal cortex (Allen et al., 2008; Schmack et al., 2013) in the genesis of perceptual symptoms and conceptually links the maintenance of delusions with top–down shaping of brain networks encoding beliefs (Allen et al., 2008; Schmack et al., 2013).

TABLE 3 Mediation analysis results for the hypothesis that symptom networks mediate the relationship between the disease network and the negative symptom in chronic dataset

X	M	Y	a path		b path		ab path	
			Z	p	Z	p	Z	p
Increased disease network	Positively related symptom network	Negative score	−1.44	.1495	3.18	.0015	−1.42	.1562
Increased disease network	Negatively related symptom network	Negative score	2.30	.0212	−3.95	<.0001	−1.95	.0517
Decreased disease network	Positively related symptom network	Negative score	0.02	.9864	3.19	.0014	0.02	.9828
Decreased disease network	Negatively related symptom network	Negative score	−1.28	.2004	−4.15	<.0001	1.33	.1842
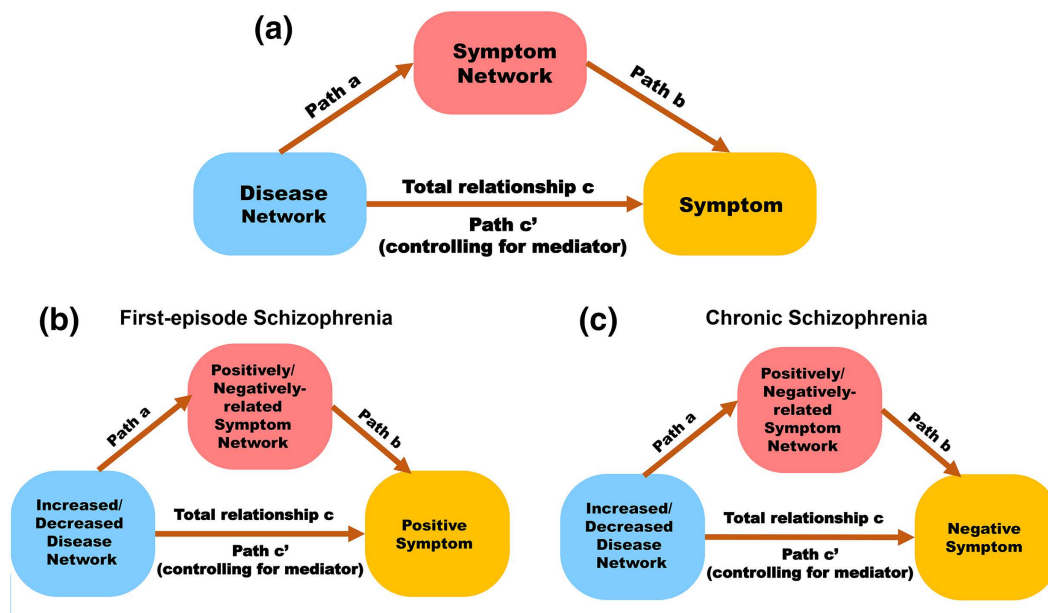
FIGURE 4 Mediation models we adopted: (a) The unified mediation model. Blue node indicates disease edges, red node indicates symptom edges and the yellow node indicates the symptom score. If the path a, path b and path a × b are all significant, we can conclude that symptom network mediate the relationship between the disease network and symptom network. (b) The mediation model for the first-episode schizophrenia dataset. As disease edges can be divided into increased/decreased group, and the symptom edges can be separated into positively/negatively related group (with positive symptom scores). Thus there are four models corresponding to the four combinations among increased/decreased disease network, positively/negatively related symptom network and positive symptom score, which are all tested. (c) The mediation model for chronic schizophrenia dataset. Four models with different combination among increased/decreased disease network, positively/negatively related symptom network (related with negative symptom scores) and negative symptom score are tested [Color figure can be viewed at wileyonlinelibrary.com]

For the patients with chronic schizophrenia, formal mediation analysis did not support a model relating disease and symptom edges and negative symptom expression directly. Differences in medication and medication history (or other environmental influences acting on the primary pathological relationships) in the chronic-stage patients may have confounded this analysis. Testing this will demand much larger populations. Nonetheless, it is worth noting that the thalamus, middle frontal gyrus, hippocampus identified in difference, and symptom networks in the chronic patients all are modulated functionally by mesocortical dopaminergic signaling, dysfunction of which has been implicated previously in negative symptomology (Goff & Evins, 1998). Dopamine, a potential final common pathway that accounts for the aberrant emotional regulation and psychosis present in the schizophrenic syndrome, plays an important role in modulating neural regions involved in emotion, cognition, and memory formation (Laviolette, 2007).

Although our work is almost unique because of the particularly large and homogenous first episode cohort, there are limitations of our study. First, a more powerful experimental design is to use two independent datasets to perform the nested-cross-validation analysis, thus using one dataset to build the prediction models and another totally independent one to test the generalizability of the models (Chen et al., 2016). However, a similarly large, independent population of first episode patients are not available for us right now. To address this limitation in part, we adopted the permutation analysis (recommend by Shen et al., 2017 for analysis with cross-validation performed within a single

dataset) to show that our prediction results are significantly better than random cases. Second, the population of chronic schizophrenic patients was relatively small and the analysis confounded by potential differences in any treatment effects. This limited the inferences that could be drawn by comparisons between results from the two cohorts. Nonetheless, our work highlighted the heterogeneity amongst patients with schizophrenia, which was our primary intention, and the need for their stratification in future studies of this kind. Third, while heuristically attractive, the bicolor graph approach is still limited by being a visualization tool, rather than a method for quantitative inference. Future work needs to integrate graph similarity measures (Zager, 2005) to test hypotheses regarding relations between disease and symptom edges in a quantitative framework. Finally, a brain network is composed of two basic elements: nodes and edges. While different definition of node (such as different brain templates) and edge (such as sparsity-based network construction (Yu et al., 2017) may result in different functional network, our approach can be applied to these networks without further adaption. The robustness of our hypothesis should be further tested under different network construction methods.

Nonetheless, bicolor graphs provide a useful method that can be applied generally for visualization of relationships between networks, for example, for exploring relationships between structural and functional disease or symptom edges in schizophrenia. As has been emphasized elsewhere recently (Wang & Krystal, 2014), approaches similar to those used here to define disease edges provide a logical basis for

biologically based diagnostic criteria that might prove more predictive of clinical course than are current, symptom based diagnoses. Our work also suggests how the brain activity characteristic of disease (reflected in the disease edges) modulates other areas of the brain for symptom expression. Definition of robust descriptions of symptom edges could guide future design of more discriminative scales for measuring symptom severity and change based on more generally defined relationships between network components and cognitive traits (Hampshire, Highfield, Parkin, & Owen, 2012). While caution is needed in making inferences about mechanism from the large-scale network models, they provide powerful tools for understanding patient heterogeneity. Their potential for pathological correlation and quantitative basis adds to their promise for clinical decision support testing in the future.

ORCID

Zhaowen Liu http://orcid.org/0000-0001-9344-8098

REFERENCES

Allen, P., Laroi, F., McGuire, P. K., & Aleman, A. (2008). The hallucinating brain: A review of structural and functional neuroimaging studies of hallucinations. *Neuroscience & Biobehavioral Reviews*, 32(1), 175–191.

Baron, R. M., & Kenny, D. A. (1986). The moderator-mediator variable distinction in social psychological research: Conceptual, strategic, and statistical considerations. *Journal of Personality and Social Psychology*, 51(6), 1173–1182.

Bhandari, A., Voineskos, D., Daskalakis, Z. J., Rajji, T. K., & Blumberger, D. M. (2016). A review of impaired neuroplasticity in schizophrenia investigated with non-invasive brain stimulation. *Frontiers in Psychiatry*, 7, 45.

Biederman, I., Glass, A. L., & Stacy, E. W. Jr. (1973). Searching for objects in real-world scences. *Journal of Experimental Psychology*, 97(1), 22–27.

Camchong, J., MacDonald, A. W., Bell, C., Mueller, B. A., & Lim, K. O. (2011). Altered functional and anatomical connectivity in schizophrenia. *Schizophrenia Bulletin*, 37(3), 640–650.

Castellanos, F. X., & Proal, E. (2012). Large-scale brain systems in ADHD: Beyond the prefrontal–striatal model. *Trends in Cognitive Sciences*, 16 (1), 17–26.

Chen, X., Zhang, H., Gao, Y., Wee, C. Y., Li, G., Shen, D., & Alzheimer's Disease Neuroimaging, I. (2016). High-order resting-state functional connectivity network for MCI classification. *Human Brain Mapping*, 37(9), 3282–3296.

Cheng, W., Palaniyappan, L., Li, M., Kendrick, K. M., Zhang, J., Luo, Q., . . . Feng, J. (2015a). Voxel-based, brain-wide association study of aberrant functional connectivity in schizophrenia implicates thalamo-cortical circuitry. *npj Schizophrenia*, 1(1), 15016.

Cheng, W., Rolls, E. T., Gu, H., Zhang, J., & Feng, J. (2015b). Autism: Reduced connectivity between cortical areas involved in face expression, theory of mind, and the sense of self. *Brain*, 138(5), 1382–1393.

Cui, H., Zhang, J., Liu, Y., Li, Q., Li, H., Zhang, L., . . . Northoff, G. (2016). Differential alterations of resting-state functional connectivity in generalized anxiety disorder and panic disorder. *Human Brain Mapping*, 37(4), 1459–1473.

Dubois, J., & Adolphs, R. (2016). Building a science of individual differences from fMRI. *Trends in Cognitive Sciences*, 20(6), 425–443.

Efron, B., & Tibshirani, R. (1993). An introduction to the Bootstrap. *Technometrics*, 37, 340–341.

Fitzgerald, P. B., Laird, A. R., Maller, J., & Daskalakis, Z. J. (2008). A meta-analytic study of changes in brain activation in depression. *Human Brain Mapping*, 29(6), 683–736.

Fornito, A., Zalesky, A., Pantelis, C., & Bullmore, E. T. (2012). Schizophrenia, neuroimaging and connectomics. *NeuroImage*, 62(4), 2296–2314.

Fox, M. D., Zhang, D., Snyder, A. Z., & Raichle, M. E. (2009). The global signal and observed anticorrelated resting state brain networks. *Journal of Neurophysiology*, 101(6), 3270–3283.

Goff, D. C., & Evins, A. E. (1998). Negative symptoms in schizophrenia: Neurobiological models and treatment response. *Harvard Review of Psychiatry*, 6(2), 59–77.

Guo, S., Kendrick, K. M., Yu, R., Wang, H. L. S., & Feng, J. (2014). Key functional circuitry altered in schizophrenia involves parietal regions associated with sense of self. *Human Brain Mapping*, 35(1), 123–139.

Hampshire, A., Highfield, R. R., Parkin, B. L., & Owen, A. M. (2012). Fractionating human intelligence. *Neuron*, 76(6), 1225–1237.

Howes, O. D., & Kapur, S. (2009). The dopamine hypothesis of schizophrenia: Version III–the final common pathway. *Schizophrenia Bulletin*, 35(3), 549–562.

Laviolette, S. R. (2007). Dopamine modulation of emotional processing in cortical and subcortical neural circuits: Evidence for a final common pathway in schizophrenia? *Schizophrenia Bulletin*, 33(4), 971–981.

Lennox, B. R., Bert, S., Park, G., Jones, P. B., & Morris, P. G. (1999). Spatial and temporal mapping of neural activity associated with auditory hallucinations. *Lancet*, 353(9153), 644.

Li, T., Wang, Q., Zhang, J., Rolls, E. T., Yang, W., Palaniyappan, L., ... Liu, Z. (2016). Brain-wide analysis of functional connectivity in first-episode and chronic stages of schizophrenia. *Schizophrenia Bulletin*, sbw099.

Liu, Y., Liang, M., Zhou, Y., He, Y., Hao, Y., Song, M., ... Jiang, T. (2008). Disrupted small-world networks in schizophrenia. *Brain*, 131(Pt 4), 945–961.

Lui, S., Deng, W., Huang, X. Q., Jiang, L. J., Ma, X. H., Chen, H. F., ... Gong, Q. Y. (2009). Association of cerebral deficits with clinical symptoms in antipsychotic-naive first-episode schizophrenia: An optimized voxel-based morphometry and resting state functional connectivity study. *American Journal of Psychiatry*, 166(2), 196–205.

Lui, S., Wu, Q., Qiu, L., Yang, X., Kuang, W., Chan, R. C., ... Gong, Q. (2011). Resting-state functional connectivity in treatment-resistant depression. *American Journal of Psychiatry*, 168(6), 642–648.

Liu, F., Guo, W., Fouche, J. P., Wang, Y., Wang, W., Ding, J., ... Chen, H. (2015). Multivariate classification of social anxiety disorder using whole brain functional connectivity. *Brain structure & function*, 220, 101–115.

Müller, R.-A., Shih, P., Keehn, B., Deyoe, J. R., Leyden, K. M., & Shukla, D. K. (2011). Underconnected, but how? A survey of functional connectivity MRI studies in autism spectrum disorders. *Cerebral Cortex*, 21(10), 2233–2243.

Mazaheri, A., Coffey-Corina, S., Mangun, G. R., Bekker, E. M., Berry, A. S., & Corbett, B. A. (2010). Functional disconnection of frontal cortex and visual cortex in attention-deficit/hyperactivity disorder. *Biological Psychiatry*, 67(7), 617–623.

McCarthy-Jones, S., Oestreich, L. K. L., Whitford, T. J., & Bank, A. S. R. (2015). Reduced integrity of the left arcuate fasciculus is specifically associated with auditory verbal hallucinations in schizophrenia. *Schizophrenia Research*, 162(1–3), 1–6.

Murphy, K., Birn, R. M., Handwerker, D. A., Jones, T. B., & Bandettini, P. A. (2009). The impact of global signal regression on resting state correlations: Are anti-correlated networks introduced? *NeuroImage*, 44(3), 893–905.

Murphy, K., & Fox, M. D. (2017). Towards a consensus regarding global signal regression for resting state functional connectivity MRI. *NeuroImage*, 154, 169–173.

Onitsuka, T., Shenton, M. E., Salisbury, D. F., Dickey, C. C., Kasai, K., Toner, S. K., ... McCarley, R. W. (2004). Middle and inferior temporal gyrus gray matter volume abnormalities in chronic schizophrenia: An MRI study. *American Journal of Psychiatry*, 161(9), 1603–1611.

Power, J. D., Mitra, A., Laumann, T. O., Snyder, A. Z., Schlaggar, B. L., & Petersen, S. E. (2014). Methods to detect, characterize, and remove motion artifact in resting state fMRI. *NeuroImage*, 84, 320–341.

Rosenberg, M. D., Finn, E. S., Scheinost, D., Papademetris, X., Shen, X., Constable, R. T., & Chun, M. M. (2016). A neuromarker of sustained attention from whole-brain functional connectivity. *Nature Neuroscience*, 19(1), 165–171.

Schmack, K., Gomez-Carrillo de Castro, A., Rothkirch, M., Sekutowicz, M., Rossler, H., Haynes, J. D., ... Sterzer, P. (2013). Delusions and the role of beliefs in perceptual inference. *Journal of Neuroscience*, 33(34), 13701–13712.

Shen, X. L., Finn, E. S., Scheinost, D., Rosenberg, M. D., Chun, M. M., Papademetris, X., & Constable, R. T. (2017). Using connectome-based predictive modeling to predict individual behavior from brain connectivity. *Nature Protocols*, 12(3), 506–518.

Simpson, E. H., Kellendonk, C., & Kandel, E. (2010). A possible role for the striatum in the pathogenesis of the cognitive symptoms of schizophrenia. *Neuron*, 65(5), 585–596.

Song, J., Desphande, A. S., Meier, T. B., Tudorascu, D. L., Vergun, S., Nair, V. A., ... Prabhakaran, V. (2012). Age-related differences in test-retest reliability in resting-state brain functional connectivity. *PLoS One*, 7(12), e49847.

Spitsyna, G., Warren, J. E., Scott, S. K., Turkheimer, F. E., & Wise, R. J. S. (2006). Converging language streams in the human temporal lobe. *Journal of Neuroscience*, 26(28), 7328–7336.

Sylvester, C., Corbetta, M., Raichle, M., Rodebaugh, T., Schlaggar, B., Sheline, Y., ... Lenze, E. (2012). Functional network dysfunction in anxiety and anxiety disorders. *Trends in Neurosciences*, 35(9), 527–535.

Tao, H., Guo, S., Ge, T., Kendrick, K. M., Xue, Z., Liu, Z., & Feng, J. (2013). Depression uncouples brain hate circuit. *Molecular Psychiatry*, 18(1), 101–111.

Tranel, D. (2009). The left temporal pole is important for retrieving words for unique concrete entities. *Aphasiology*, 23(7–8), 867–884.

Tzourio-Mazoyer, N., Landeau, B., Papathanassiou, D., Crivello, F., Etard, O., Delcroix, N., ... Joliot, M. (2002). Automated anatomical labeling of activations in SPM using a macroscopic anatomical parcellation of the MNI MRI single-subject brain. *NeuroImage*, 15(1), 273–289.

Wager, T. D., Davidson, M. L., Hughes, B. L., Lindquist, M. A., & Ochsner, K. N. (2008). Prefrontal-subcortical pathways mediating successful emotion regulation. *Neuron*, 59(6), 1037–1050.

Wang, X. J., & Krystal, J. H. (2014). Computational psychiatry. *Neuron*, 84(3), 638–654.

Yu, R., Zhang, H., An, L., Chen, X., Wei, Z., & Shen, D. (2017). Connectivity strength-weighted sparse group representation-based brain network construction for MCI classification. *Human Brain Mapping*, 38(5), 2370–2383.

Zager, L. (2005). *Graph similarity and matching*. Massachusetts Institute of Technology.

Zhang, J., Kendrick, K. M., Lu, G., & Feng, J. (2015). The fault lies on the other side: Altered brain functional connectivity in psychiatric disorders is mainly caused by counterpart regions in the opposite hemisphere. *Cerebral Cortex*, 25(10), 3475–3486.

SUPPORTING INFORMATION

Additional Supporting Information may be found online in the supporting information tab for this article.